Supplementary data

Paolo Oliva,*[a] Benjamin Andreas Bircher,[a,b] Cora-Ann Schoenenberger [c] and Thomas Braun[a]

[a] *Center for Cellular Imaging and Nanoanalytics (C-CINA), University of Basel, Mattenstrasse 26, Basel, Switzerland. E-mail: paolo.oliva@unibas.ch, thomas.braun@unibas.ch*

[b] *Current address: Federal Institute of Metrology, Lindenweg 50, Bern-Wabern, Switzerland. E-mail: benjamin.bircher@metas.ch*

[c] *Department of Chemistry, University of Basel, Mattenstrasse 24a, Basel, Switzerland. E-mail: cora-ann.schoenenberger@unibas.ch*

Contents

1 Reference viscosities and mass densities

The reference viscosities were measured using a rolling ball viscometer (AMVn Viscometer, Anton Paar, Switzerland) consisting of a capillary 1.6 mm in diameter and a ball with a density of 7.65 g cm^{-3}. The measurements were performed for different tilt angles (50°, 60°, and 70°) and four repeats per sample and angle.

For the determination of the reference mass densities, a density meter (DMA 4500, Anton Paar, Switzerland) was used. A temperature of 20 °C was set for all measurements.

Table 1: Reference viscosities and mass densities of water and glycerol solutions. For low viscous fluids (0 mPa s–6.63 mPa s) the calibration fluids are marked with an asterisk. For high viscous fluids (13.16 mPa s–219 mPa s) the used reference liquids are marked with a circle. The viscosity of 85 %- and 90 %-glycerol are theoretical values. The determination by the classical Anton Paar viscometer was not possible due to high rolling time.

Sample /% V/V	Density /kg m^{-3}	Viscosity /mPa s	ROM
0	998.21	0.9972	*
10	1031.81	1.4494	
20	1050.57	1.8358	
25	1065.72	2.2514	
30	1079.18	2.6715	* ○
35	1094.54	3.4054	
40	1106.52	4.1846	
45	1117.88	5.2058	
50	1132.53	6.6252	*
60	1163.66	13.1617	○
85	1220.85	109	
90	1232.1	219	○

2 General model description

2.1 Derivation of the driven damped harmonic oscillator model in relation to the ROM

For calibration of the viscosity and liquid density platform, a reduced order model (ROM) has been applied. This model was tested for several resonators with different geometries [1]. Geometrical, material and measurement-platform dependent parameters are not explicitly incorporated but taken into consideration by a calibration step.

The ROM considers a linear, mechanical oscillator with a lumped mass m_0, a damping coefficient c_0 and a spring constant k_0 fully immersed in a liquid. This model is governed by the following differential equation:

$$m_0 \frac{\mathrm{d}}{\mathrm{d}t} \frac{\mathrm{d}x(t)}{\mathrm{d}t} + c_0 \frac{\mathrm{d}x(t)}{\mathrm{d}t} + k_0 x(t) = F_{drive}(t) - F_{fluid}(t) \tag{1}$$

where F_{drive} is the time-dependent external driving force, F_{fluid} the force exerted by the fluid and $x(t)$ the time-dependent displacement function of the lumped mass. This equation describes a driven damped harmonic oscillator (DDHO). The fluid force is described by the following term:

$$F_{fluid}(t) = c_f \frac{\mathrm{d}x}{\mathrm{d}t} + m_f \frac{\mathrm{d}}{\mathrm{d}t}\frac{\mathrm{d}x}{\mathrm{d}t} \tag{2}$$

where c_f is the damping coefficient of the fluid and m_f the co-moving fluid mass. The simplified expressions for the resonance frequency and for the quality factor are derived from eq. (1) and listed below:

$$f_{exp} \approx \frac{1}{2\pi\sqrt{m_{0k} + m_{\rho k} * \rho + m^*_{\eta\rho k} * \sqrt{\eta\,\rho}}}\,, \tag{3}$$

$$Q_{exp} \approx \frac{\sqrt{m_{0k} + m_{\rho k} * \rho + m^*_{\eta\rho k} * \sqrt{\eta\,\rho}}}{c_{0k} + c_{\eta k} * \eta + c^*_{\eta\rho k} * \sqrt{\eta\,\rho}} \tag{4}$$

By measuring the eigenfrequency and the quality factor of three known liquids we can determine the required six coefficients, m_{0k}, $m_{\rho k}$, $m^*_{\eta rhok}$, c_{0k}, $c_{\eta k}$ and $c^*_{\eta\rho k}$.

f_{exp} and Q_{exp} are the measured eigenfrequency and quality factor of the analyzed liquid. In our case, this equation system has been implemented in Wolfram Mathematica, which first calculates the resulting fluid properties and then shows the results in two separated 3D maps. These maps give information about the validity of the calculated ROM coefficients (graphs shown below).

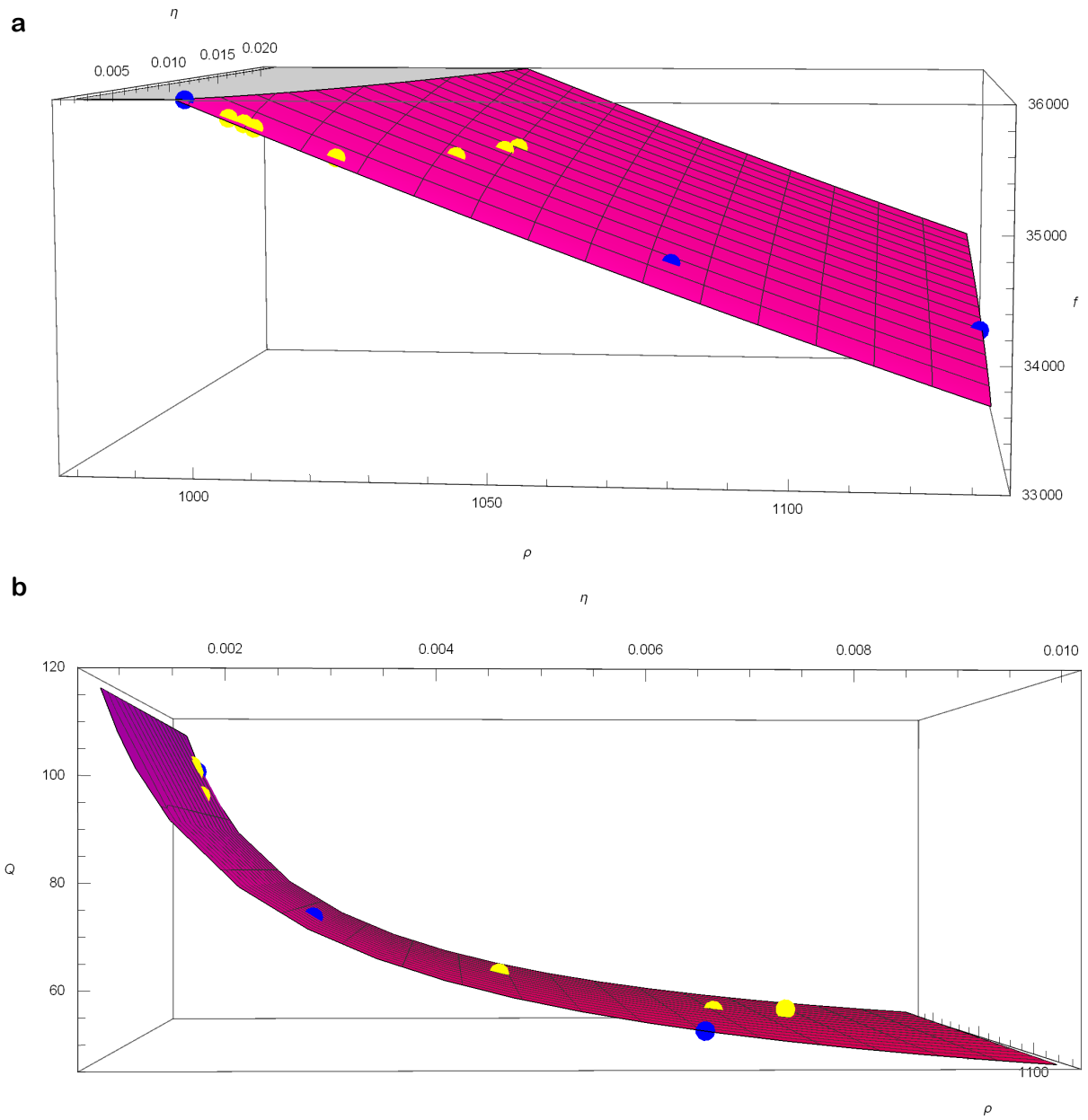

Figure 1: Resulting calibration planes for the measured eigenfrequencies (a) and quality factors (b) for corresponding mass densities and dynamic viscosities. The blue circles represent the three calibration fluids, and the yellow ones are the measured actin solutions.

2.2 Limitation of the reduced order model

To establish a well-defined plane, it is essential to choose fluids which are well distributed; this means that the viscosities and mass densities of the calibration liquids should have significant deviations from each other. Additionally, it is necessary to use always the same calibration fluids otherwise a comparison of the results can lead to incorrect interpretation. A discrepancy in the fluid properties between two different measurement series calibrated with different liquids has primarily been observed in the resulting liquid density. Deviations in the chosen liquid viscosities seem to affect less the distance between two calibration planes (see figure below).

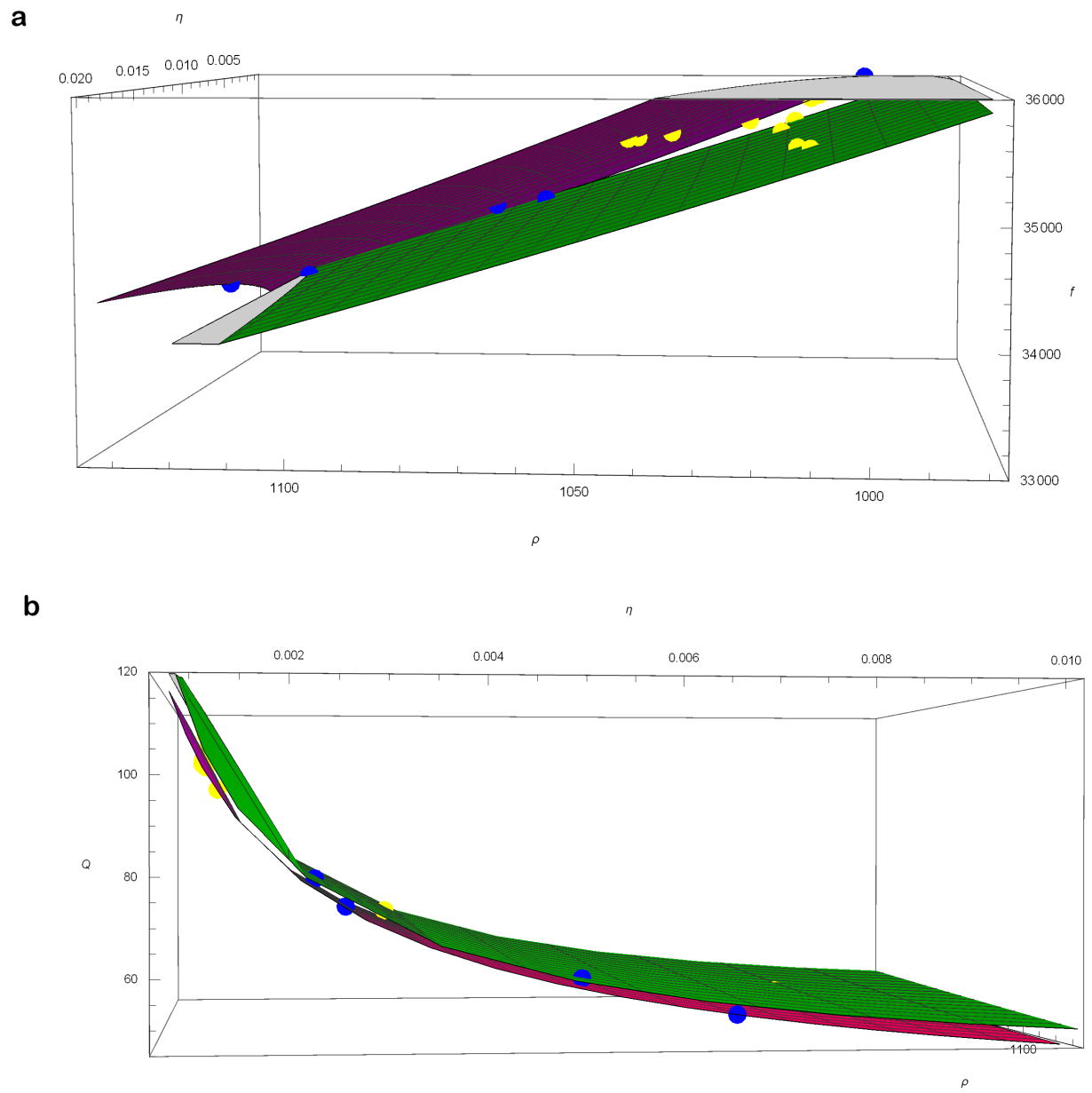

Figure 2: Analysis of resulting discrepancy between different calibration fluids (a) for corresponding mass density and (b) viscosity. Blue circles represent the calibration liquids.

2.3 Calculation of ROM coefficients

To determine the viscosities and mass densities from eigenfrequency and quality factor with the reduced order model a calibration step is needed. This step is performed before every measurement. For each sample the corresponding amplitude and phase curves were measured and by fitting (Levenberg-Marquardt algorithm implemented in Igor Pro) a driven damped harmonic oscillator model to the data, the eigenfrequencies and the quality factors were determined. These parameters are finally inserted into a linear least square equation to calculate the calibration coefficients (see ch. 2.1).

Table 2: Measured eigenfrequencies and quality factors of water and glycerol solutions (fitted value ± SD). The fluids marked with an asterisk were used to calculate the ROM coefficients (listed in table 3), and from the remaining liquids, viscosities and mass densities were calculated by applying the reduced order model.

Sample	f_{exp} [kHz]	Q_{exp}	Calibration ROM
0 %	35.335 ± 1.24	116.25 ± 1.07	*
10 %	34.872 ± 0.871	98.002 ± 0.624	
20 %	34.540 ± 1	89.014 ± 0.591	
25 %	34.223 ± 1	82.844 ± 0.532	
30 %	34.047 ± 1.27	78.266 ± 0.573	*
35 %	33.799 ± 1.24	70.855 ± 0.478	
40 %	33.688 ± 1.39	68.457 ± 0.473	
45 %	33.492 ± 1.83	61.234 ± 0.431	
50 %	33.350 ± 1.81	56.813 ± 0.428	*

Table 3: ROM coefficients calculated for the experiments shown in Fig. 5a.

$$
\begin{aligned}
m_{0k} &= -1.3085 \times 10^{-12}\,\mathrm{s}^2 \\
m_{\rho k} &= 2.1889 \times 10^{-14}\,\mathrm{m}^3\,\mathrm{s}^2\,\mathrm{kg}^{-1} \\
m^*_{\eta\rho k} &= -2.5389 \times 10^{-13}\,\mathrm{m}^2\,\mathrm{s}^{5/2}\,\mathrm{kg}^{-1} \\
c_{0k} &= 4.0390 \times 10^{-9}\,\mathrm{s} \\
c_{\eta k} &= -3.4906 \times 10^{-6}\,\mathrm{m}\,\mathrm{s}^2\,\mathrm{kg}^{-1} \\
c^*_{\eta\rho k} &= 3.8275 \times 10^{-8}\,\mathrm{m}^2\,\mathrm{s}^{3/2}\,\mathrm{kg}^{-1}
\end{aligned}
$$

Table 4: Measured eigenfrequencies and quality factors of high viscous fluids. The fluids marked with a circle were used to determine the ROM coefficients listed in table 5.

Sample	f_{exp} [kHz]	Q_{exp}	Calibration ROM
30 %	34.715	65.627	∘
60 %	33.459	46.986	∘
85 %	32.836	27.261	
90 %	32.593	24.904	∘

Table 5: ROM coefficients calculated for the determination of the liquid properties of high viscous fluids shown in Fig. 5b.

$$
\begin{aligned}
m_{0k} &= 1.8756 \times 10^{-12}\,\mathrm{s}^2 \\
m_{\rho k} &= 1.7869 \times 10^{-14}\,\mathrm{m}^3\,\mathrm{s}^2\,\mathrm{kg}^{-1} \\
m^*_{\eta\rho k} &= -6.1516 \times 10^{-15}\,\mathrm{m}^2\,\mathrm{s}^{5/2}\,\mathrm{kg}^{-1} \\
c_{0k} &= 3.236\,03 \times 10^{-9}\,\mathrm{s} \\
c_{\eta k} &= -1.8444 \times 10^{-6}\,\mathrm{m}\,\mathrm{s}^2\,\mathrm{kg}^{-1} \\
c^*_{\eta\rho k} &= 3.6285 \times 10^{-8}\,\mathrm{m}^2\,\mathrm{s}^{3/2}\,\mathrm{kg}^{-1}
\end{aligned}
$$

Table 6: Measured eigenfrequencies and quality factors used to calculate the ROM coefficients presented in table 7.

Sample	f_{exp} [kHz]	Q_{exp}
0 %	35.713	110.21
30 %	34.291	72.50
50 %	33.558	53.95

Table 7: ROM coefficients calculated for the experiments presented in Fig. 6a.

$$
\begin{aligned}
m_{0k} &= -3.6653 \times 10^{-12}\,\mathrm{s}^2 \\
m_{\rho k} &= 2.3934 \times 10^{-14}\,\mathrm{m}^3\,\mathrm{s}^2\,\mathrm{kg}^{-1} \\
m^*_{\eta\rho k} &= -3.6649 \times 10^{-13}\,\mathrm{m}^2\,\mathrm{s}^{5/2}\,\mathrm{kg}^{-1} \\
c_{0k} &= -3.7631 \times 10^{-9}\,\mathrm{s} \\
c_{\eta k} &= -7.6355 \times 10^{-6}\,\mathrm{m}\,\mathrm{s}^2\,\mathrm{kg}^{-1} \\
c^*_{\eta\rho k} &= 5.1932 \times 10^{-8}\,\mathrm{m}^2\,\mathrm{s}^{3/2}\,\mathrm{kg}^{-1}
\end{aligned}
$$

Table 8: Measured eigenfrequencies and quality factors of the calibration fluids used to determine the ROM coefficients presented in table 9.

Sample	f_{exp} [kHz]	Q_{exp}
0 %	35.719	117.87
30%	34.373	78.619
50%	33.712	57.669

Table 9: Calculated ROM coefficients for the experiment shown in Fig. 6b.

$$
\begin{aligned}
m_{0k} &= -2.296\,83 \times 10^{-12}\,\mathrm{s}^2 \\
m_{\rho k} &= 2.253\,15 \times 10^{-14}\,\mathrm{m}^3\,\mathrm{s}^2\,\mathrm{kg}^{-1} \\
m^*_{\eta\rho k} &= -3.413\,66 \times 10^{-13}\,\mathrm{m}^2\,\mathrm{s}^{5/2}\,\mathrm{kg}^{-1} \\
c_{0k} &= -1.035\,91 \times 10^{-10}\,\mathrm{s} \\
c_{\eta k} &= -5.656\,82 \times 10^{-6}\,\mathrm{m}\,\mathrm{s}^2\,\mathrm{kg}^{-1} \\
c^*_{\eta\rho k} &= 3.3647 \times 10^{-8}\,\mathrm{m}^2\,\mathrm{s}^{3/2}\,\mathrm{kg}^{-1}
\end{aligned}
$$

3 Typical sweeper analysis of a G-actin polymerization

Fig. 3 shows a typical amplitude and phase curve of a G-actin polymerization. After a steady-state is achieved PolyMix is added to the solution and a significant frequency shift is visible. In addition, over time the amplitude starts to decrease which coincides with a decreasing slope of the phase curve. This is related to the formation of filamentous actin.

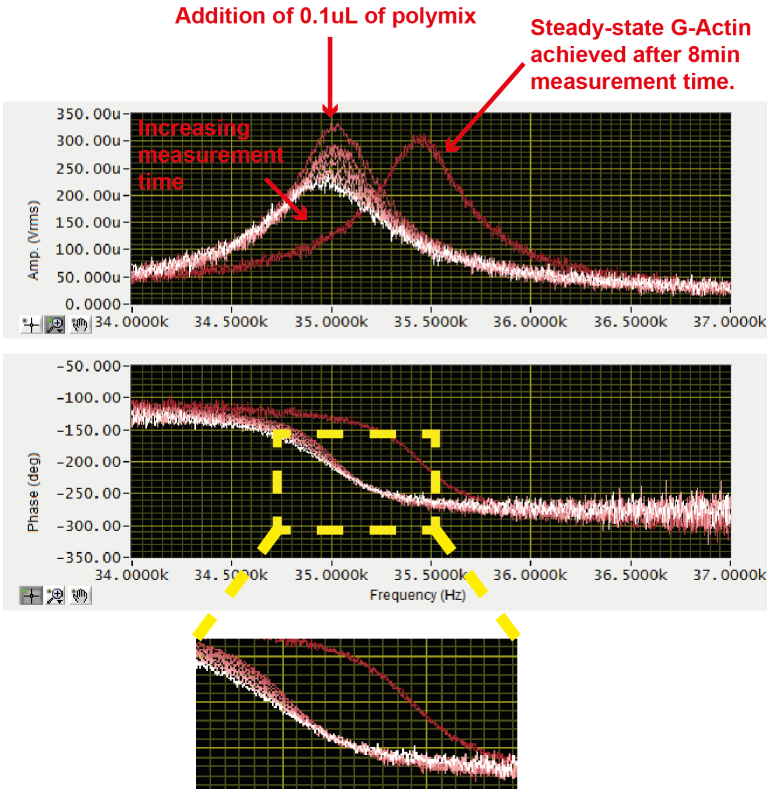

Figure 3: Amplitude and phase curves collected during the G-Actin polymerization.

4 G-actin polymerization measured with different silicon-nitride membranes

To prove the membrane independence of the G-actin polymerization, the same experiment presented in the main article (ch. 3.3) has been performed with different membranes.

As we can see from the graphs (Fig. 4) different viscosity and mass density maxima can be achieved. This is also pointed out from the different measured eigenfrequencies.

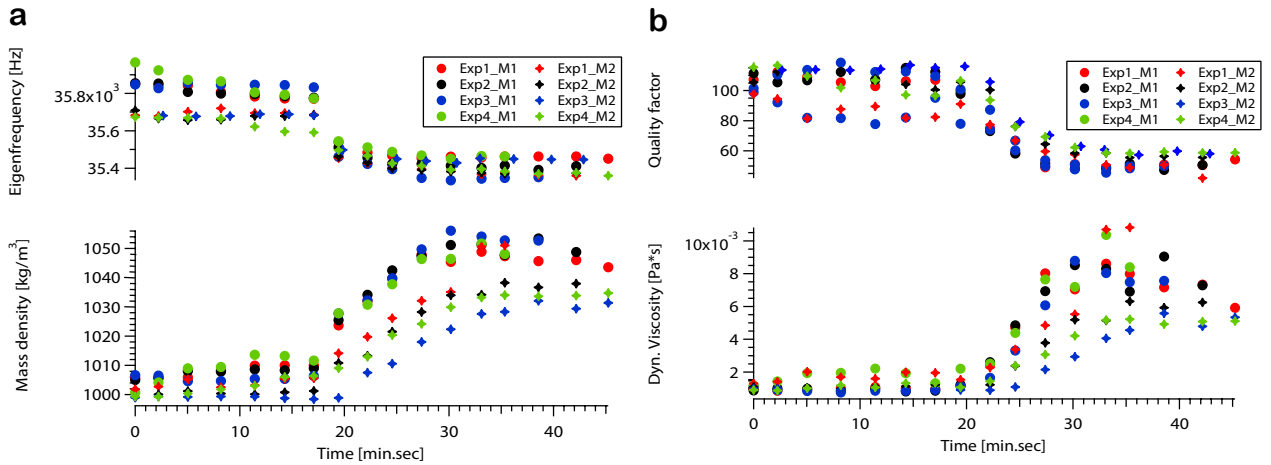

Figure 4: (a) Graphs show the measured eigenfrequencies and the calculated mass densities. Each color stands for one experiment, and each marker represents one silicon-nitride membrane. *M1* and *M2* stand for two different used Si_3N_4-membrane having the same physical properties; (b) Plots show the measured Q-factors and the corresponding calculated viscosities. Fluid properties have been measured with the reduced order model.

5 Typical data analysis workflow

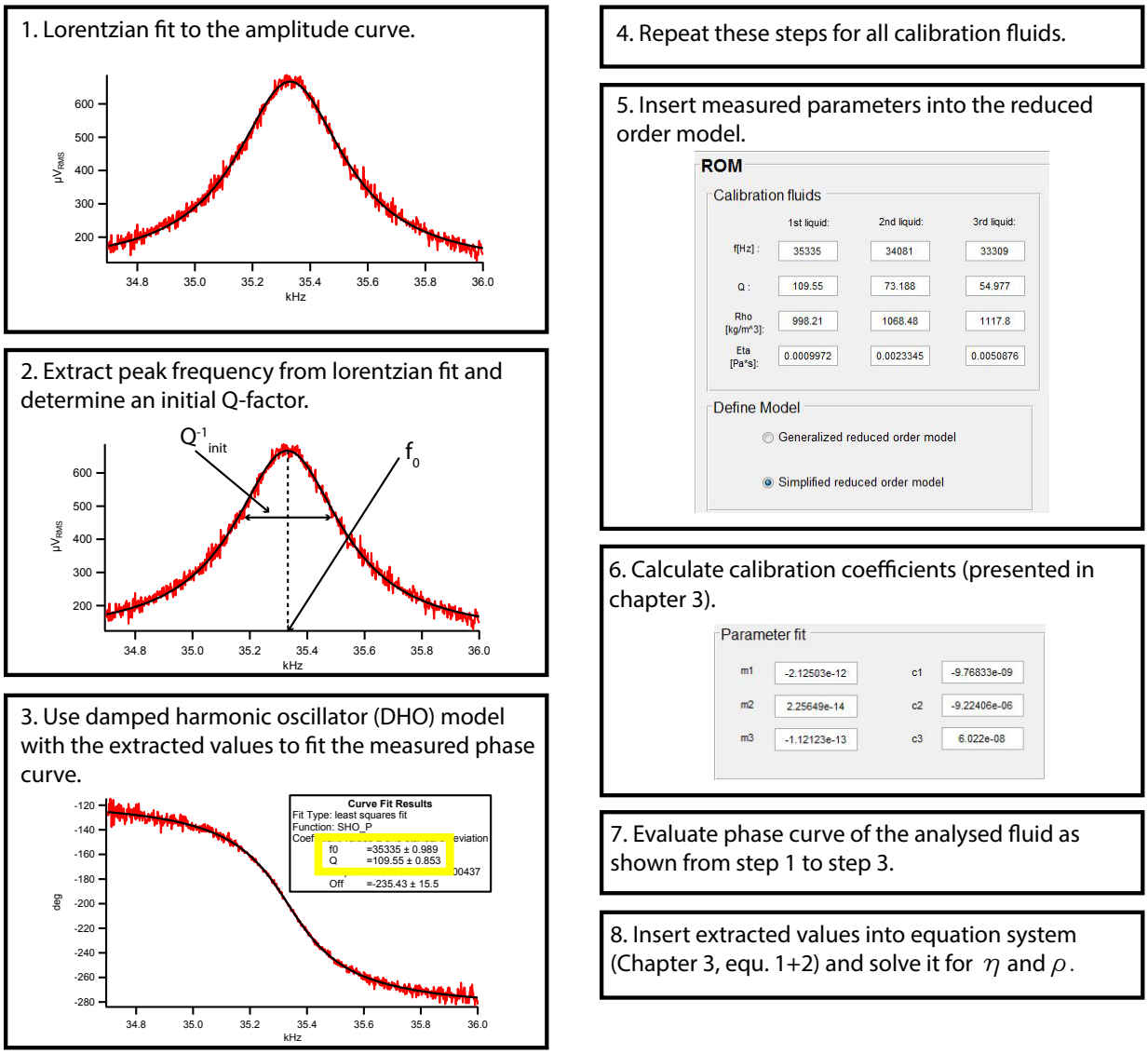

Figure 5: Workflow of the data analysis part.

6 Calculation of the phonon band diagram of silicon-nitride membranes

To analyze the clamping loss induced by the coupling of the membrane and its support, a phonon dispersion relation analysis of a commercially available Si_3N_4-membrane in COMSOL Multiphysics® was performed. The model consists of two rectangulars with different lengths and widths. In our particular case these geometries were built with the same dimensions as the membranes used in our experiments. The material properties were taken from the COMSOL library, and the solid mechanics module, coupled with an eigenfrequency analysis, was used. As periodic boundary condition a Floquet periodicity with corresponding k-vectors was considered.

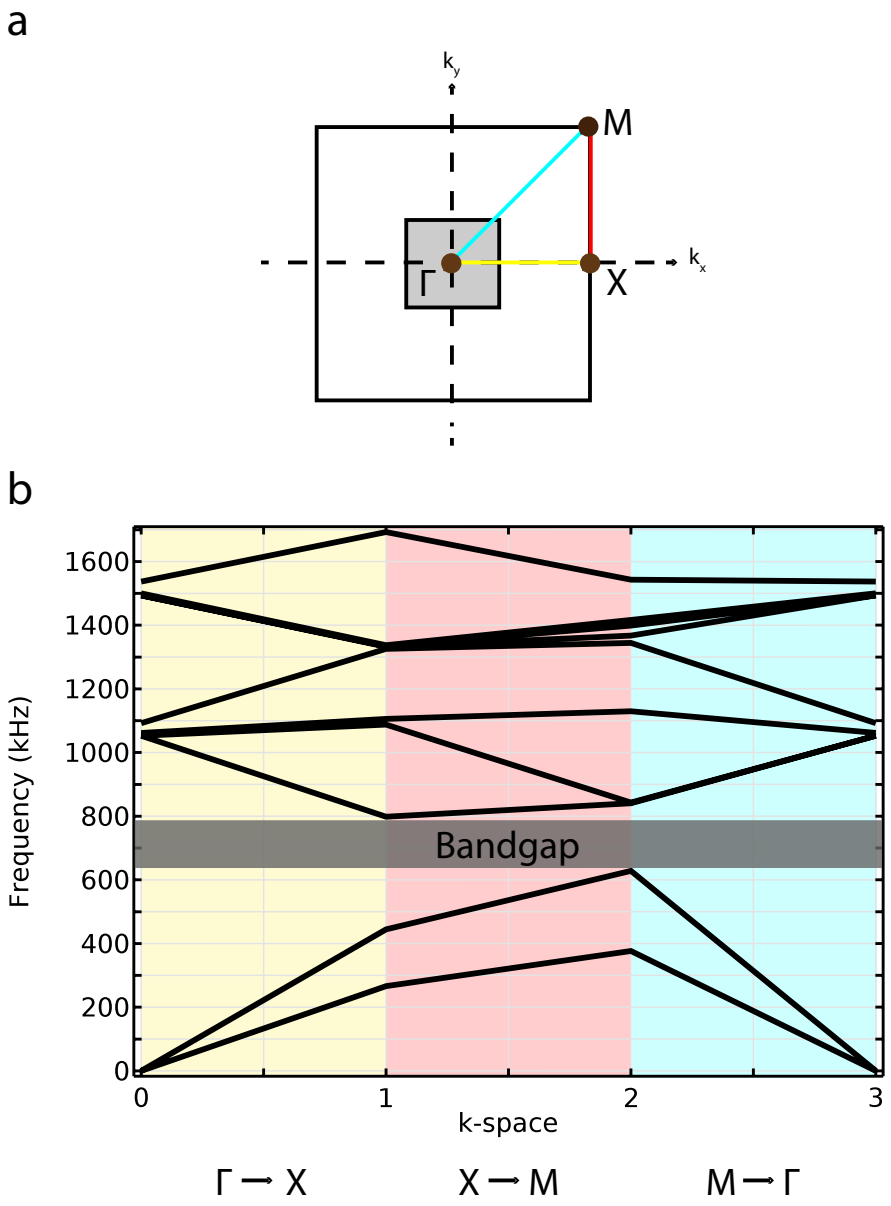

Figure 6: Results of the simulated phonon dispersion relation in COMSOL Multiphysics®. (a) Geometries of the used Si_3N_4-membranes. The blue square is the silicon frame and the central gold part is the Si_3N_4-layer. Both components were considered to be the first Brillouin zone (primitive unit cell in the reciprocal space). The Γ-point was set in the middle of the the Si_3N_4-frame; (b) Simulated phonon dispersion relation of the used Si_3N_4-membranes. For the simulation the k-space was divided into three parts: $\Gamma \rightarrow X$ goes from 0 to 1 (yellow part), $X \rightarrow M$ from 1 to 2 (red part) and $M \rightarrow \Gamma$ from 2 to 3 (light blue part). The gray part shows the calculated phononic bandgap.

References

[1] M. Heinisch, E. K. Reichel, I. Dufour, and B. Jakoby. Modeling and experimental investigation of resonant viscosity and mass density sensors considering their cross-sensitivity to temperature. *Procedia Engineering*, 87:472–475, 2014.